Model Predictive Control Approach for Real-time Control of Detention Ponds: Balancing Flood Control and Water Quality Treatment

Marcus Nóbrega Gomes Jr.[a,b,c], Luis Miguel Castillo Rápallo[a], Ahmad F. Taha[d], Eduardo Mario Mendiondo[a], Marcio Hofheinz Giacomoni[b]

[a] *University of São Paulo, Department of Hydraulic Engineering and Sanitation, São Carlos School of Engineering, Av. Trab. São Carlense, 400 - Centro, São Carlos, 13566-590, São Paulo, Brazil*

[b] *University of Texas at San Antonio, College of Engineering and Integrated Design, School of Civil & Environmental Engineering and Construction Management, One UTSA Circle, BSE 1.310, San Antonio, 78249, Texas, United States of America*

[c] *University of Arizona, Department of Hydrology and Atmospheric Sciences, James E. Rogers Way, 316A, Tucson, 85719, Arizona, United States of America*

[d] *Vanderbilt University, Department of Civil and Environmental Engineering, Jacobs Hall, Office # 293, 24th Avenue South, Nashville, 37235, Tennessee, United States of America*

1. Supplemental Information

1.1. Model Boundary Condtions

During the transition between wet weather and dry weather periods, soil water availability might change the dynamics of the flow routing. Therefore, we present two internal boundary conditions when the available soil moisture is not enough for evapotranpisration and groundwater replenishing. Twi differential equations are solved: one in the interface between the soil and the atmosphere and other for the interaction between underlying soils with the wetting front.

During dry periods, ETP tends to increase and the soil content is lost due to surface and sub-surface fluxes. Therefore, during dry periods, there is a conflict of water availability. Therefore, we calculate the infiltration rate as the soil flux at the surface, which can be written as follows:

$$f(k+1) = \min\left[\frac{h(k)}{\Delta t} + i(k) + \Delta q(k) - e_{\mathrm{TR}}, \mathrm{k_{sat}}\Big(\frac{\Delta\theta(h(k)+\psi)}{f_{\mathrm{d}}(k)}\Big)\right], \quad (1)$$

where k_{sat} is the saturated hydraulic conductivity, $\Delta q = q_{\text{in}} - q_{\text{out}}$, and $\Delta\theta$ is the soil moisture deficit.

The infiltration rate value can become negative during dry periods, and it influences the soil moisture mass balance equation. As aforementioned, during the transition between a wet cell (i.e., $h(k) > 0$) to a dry cell, that is, when the calculation of $h(k+1)$ becomes negative, the flux f is no longer given by (1), such that we ensure that $h(k+1) = 0$ as follows:

$$f(k+1) = \frac{h(k)}{\Delta t} - i(k) - \Delta q(k) - e_{\text{TR}} \tag{2}$$

Moreover, if the sub-surface depth of the wetting front becomes smaller than a threshold $f_d^{\min}$, we change the groundwater replenishing rate by fixing $f_d(k+1) = f_d^{\min}$, resulting in:

$$f_{\text{g}}(k+1) = f(k) - \frac{(f_d^{\min} - f_d(k))}{\Delta t} \tag{3}$$

In (3), numerical issues can occur if $f(k) < 0$, that is, if the soil flux at the surface is oriented upward, mainly due to evapotranspiration, which would result in a negative groundwater replenishing rate. Therefore, we implement a boundary at $f_{\text{g}}(k+1)$ resulting in a minimum f_{g} of 0. In these cases, the infiltration flux f is solved by substituting $f_{\text{g}}(k+1) = 0$ into (3).

1.2. Green-Ampt Infiltration Model

The infiltration capacity used in the model is the Green-Ampt infiltration model [1], which considers a sharp wetting front with a constant pressure equals the suction head ψ, which is movable downwards if infiltration keeps occurring. The general expression for the infiltration capacity for a given cell (i, j) in the domain is expressed as follows:

$$C_f^{\text{i,j}}(t) = k_{\text{sat}}^{i,j}\left[1 + \frac{(\psi^{i,j} + d^{i,j}(t))}{L^{i,j}(t)}\right] \tag{4}$$

where $C_f^{i,j}(t)$ is the infiltration capacity (LT^{-1}), $k_{\text{sat}}^{i,j}$ is the saturated hydraulic conductivity (LT^{-1}), $L(t) = \frac{F_d(t)}{\Delta\theta}$ is the wetting front depth (L), and $\psi^{i,j}$ is the suction head (L).

The infiltration rate is the minimum value between the infiltration capacity and the water availability rate and can be calculated for a time $t + \Delta t$ with inflow rates, depths, and infiltrated depths from t.

1.3. Evapotranspiration Model

Although not often considered in rapid and intense flood modeling, evapotranspiration (ET) is important in continuous simulation models. ET is the process of evaporation in the soil plant system that transfers water into the atmosphere [2]. Several models are available to estimate the reference evapotranspiration (E_{to}) flux in monthly [3], daily [4], or even sub-daily scale [5]. The input data required to simulate ET varies, and the proper selection of the model should be done according to the availability of data in the catchment. In this paper, we use the Penman-Monteith model, which requires spatialized data of wind speed at 2 m from surface, relative humidity, temperature, and radiation. These variables can be indirectly estimated as described in the Supplemental Material using the FAO method [6].

Let (i, j) collect the central coordinates of a specific cell. The rate of evapotranspiration can be estimated as follows:

$$e_{\mathrm{TP}}^{\mathrm{i,j}} = \frac{0.408 \times \Delta^{\mathrm{i,j}}(r_{\mathrm{n}}^{\mathrm{i,j}} - g^{\mathrm{i,j}}) + \gamma^{\mathrm{i,j}} \times \frac{900}{t^{\mathrm{i,j}}+273} \times u_2^{\mathrm{i,j}} \times (e_{\mathrm{s}}^{\mathrm{i,j}} - e_{\mathrm{a}}^{\mathrm{i,j}})}{\Delta^{\mathrm{i,j}} + \gamma^{\mathrm{i,j}} \times (1 + 0.34 \times u_2^{\mathrm{i,j}})}, \tag{5}$$

where $\Delta^{\mathrm{i,j}}$ = slope vapor pressure curve ($\mathrm{kPa}^{\circ} \cdot \mathrm{C}^{-1}$), $\mathrm{r}_{\mathrm{n}}^{\mathrm{i,j}}$ = net radiation at the crop surface ($\mathrm{MJ} \cdot \mathrm{m}^{-2} \cdot \mathrm{day}^{-1}$), $g^{\mathrm{i,j}}$ = soil heat flux ($\mathrm{MJ} \cdot \mathrm{m}^{-2} \cdot \mathrm{day}^{-1}$), $\gamma^{\mathrm{i,j}}$ = psychometric constant ($\mathrm{kPa}^{\circ} \cdot \mathrm{C}^{-1}$), $t^{\mathrm{i,j}}$ = mean daily air temperature at 2 m height in (°C), $u_2^{\mathrm{i,j}}$ = wind speed at 2 m height ($\mathrm{m} \cdot \mathrm{s}^{-1}$), $e_s^{\mathrm{i,j}}$ = saturation vapor pressure (kPa) and $e_a^{\mathrm{i,j}}$ = actual vapor pressure (kPa).

1.4. Soil Recover and Groundwater Replenishing

Three hydrological processes are assumed to occur in the soil media. The evapotranspiration and sub-surface drainage reduce the water content in the media, whereas infiltration from the upper zone increases it. We focus here on the methods to estimate f_g, which depends on the replenishing rate k_{r} and on the uppermost layer depth l_u, written as [7]:

$$k_{\mathrm{r}} = \frac{\sqrt{k_{\mathrm{sat}}/25.4}}{75} \tag{6}$$

$$t_{\mathrm{r}} = \frac{4.5}{\sqrt{k_{\mathrm{sat}}/25.4}} \tag{7}$$

$$l_{\mathrm{u}} = 4\sqrt{k_{\mathrm{sat}}/25.4}, \tag{8}$$

where k_{r} = replenishing rate (h^{-1}), t_{r} = recovery time (h), and l_{u} = uppermost layer depth (m).

From previous equations, we can infer that the subsurface exfiltration rate is given by:

$$f_{\mathrm{g}} = (\theta_{\mathrm{sat}} - \theta_{\mathrm{i}}) k_{\mathrm{r}} l_{\mathrm{u}} 1000 \tag{9}$$

where f_{g} = subsurface exfiltration rate ($\mathrm{mm} \cdot \mathrm{h}^{-1}$), θ_{sat} = saturated soil content ($-$), and θ_i = initial soil content ($-$). Therefore, f_{g} is a constant subsurface exfiltration rate applied in the water balance equation.

The supplemental material contains more information about some boundary conditions required in the model during issues that might occur during wetting / drying computational time-steps. In brief, the model identifies such cases and distributes the available soil moisture and evapotranspiration rates to conserve the mass balance. Moreover, the calculation of the real evapotranspiration is also described in the supplemental material section.

1.5. Stage-Area-Volume Functions Derivation

Let n_{s} be the number of points with known area and stage values. Let also h_{s} be the number of known stages such that $\boldsymbol{h}_{\mathrm{s}} = [0,\ h_{\mathrm{s,1}},\ h_{\mathrm{s,2}}, \ldots,\ h_{\mathrm{n_s}}]^{\mathrm{T}}$ and the associated area values of these stages are given by $\boldsymbol{\omega}_{\mathrm{s}} = [\omega_1,\ \omega_2, \ldots,\ \omega_{\mathrm{n_s}}]^{\mathrm{T}}$. We automatically derive a volume function by integrating the following expression:

$$A(h)_{\mathrm{i+1}} = A(h)_{\mathrm{i}} + \left(\frac{\mathrm{d}A}{\mathrm{d}h}\right)_i (h - h_{\mathrm{s,i}}),\ \forall\ i = 1, 2, \cdots n_{\mathrm{s}} \tag{10}$$

The derivative of the area in terms of the stage is calculated by a simple rate of change of the area with the rate of the change in the stage and is updated for each stage interval starting from the invert of the reservoir up to the final point at its top. Therefore, if there is n_{s} stage x area points, we derive $n_{\mathrm{s}-1}$ functions of area with respect to the depth.

By integrating the area over the water depth, one can derive the reservoir volume function, such that:

$$\omega_{\mathrm{r}}(h)_{i+1} = \omega_{\mathrm{r}}(h)_i + \int_{h_{\mathrm{s,i}}}^{h} A(h)_i \eta_i(h) \mathrm{d}h,\ \forall\ i = 1, 2, \cdots n_{\mathrm{s}} \tag{11}$$

where $\eta := g\left(h^{\mathrm{r}}(k)\right)$ is the reservoir depth-porosity function.

In Matlab, Eq. (11) is solved with symbolic expressions automatically, allowing the derivation for different area-functions with varied number of known stages.

1.6. Spatial Interpolation of Climatologic Variables

Given a n_s number of stations, we store the station values for a given time t in $\boldsymbol{z}_\mathrm{s}(t) = [z_\mathrm{s}^1(t),\ z_\mathrm{s}^2(t), \ldots z_\mathrm{s}^{n_\mathrm{s}}(t)]^\mathrm{T}$ with the stations located at known projected coordinates x and y described by vectors $\boldsymbol{x}_\mathrm{s}$ and $\boldsymbol{y}_\mathrm{s}$, respectively. Therefore, we can apply the IDW method [8] by calculating the distances within stations and the coordinates of each point of the spatial grid of the catchment, as follows:

$$\hat{z}(\mathbf{x}_\mathrm{s}, \mathbf{y}_\mathrm{s}) = \frac{\sum_i^{n_c} w_i z_\mathrm{s}^i}{\sum_i^n w_i},\ w_i = ||(\mathbf{x}_\mathrm{s}, \mathbf{y}_\mathrm{s}) - (\mathbf{x_i}, \mathbf{y_i})||_2^{-\beta} \tag{12}$$

where n_c is the number of cells in the catchment, β is the weightning factor and is asssumed equals 2 in this paper to represent the Euclidean distance.

We apply (12) for all cells of the catchment domain for (i) rainfall intensity, (ii) maximum temperature, (iii) minimum temperature, (iv) average temperature, (iv) wind speed at 2 m height, (v) relative humidity, and solar radiation. These interpolated climatologic variables allow to estimate rainfall intensity and evapotranspiration modeled with Pennan-Monteith (PE) method spatially. More details of the governing equations for the PE method can be found in the Supplemental Material of the research conducted in [9].

1.7. RTC-Stormwater Adopted Parameters for the Simulation

The MPC and RTC-SM parameters used in the simulations are described in Tab. 1.

1.8. 1-yr continuous simulation passive results

We discretize the events into 3 particular cases. The first one corresponds to the days 276 to 278 and represent a minor flood event. The second one is represented by days 80 to 120 and display a case of a composite flood event during a wet weather period. Finally, a large flood period is shown from days 160 to 190.

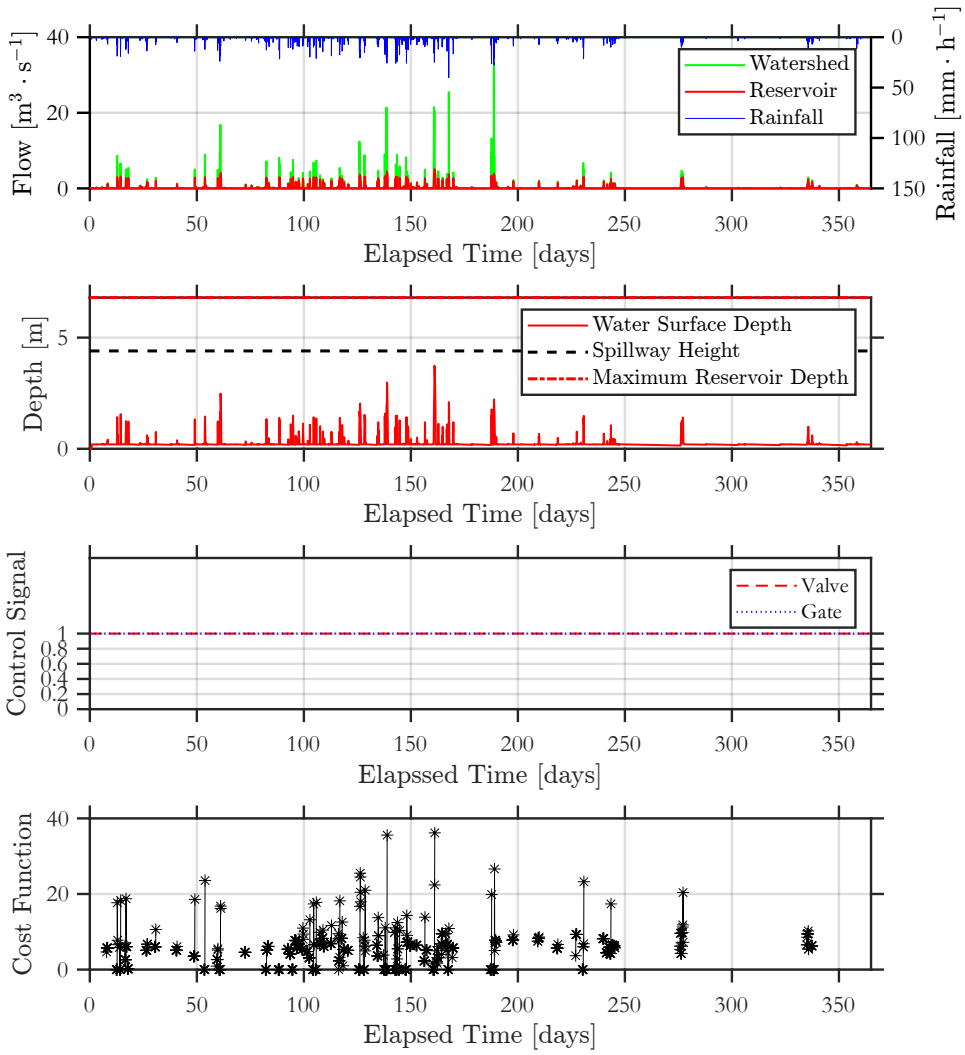

Figure 1: Continuous simulation results for day 1 to 365 of the passive scenario with valves fully opened.

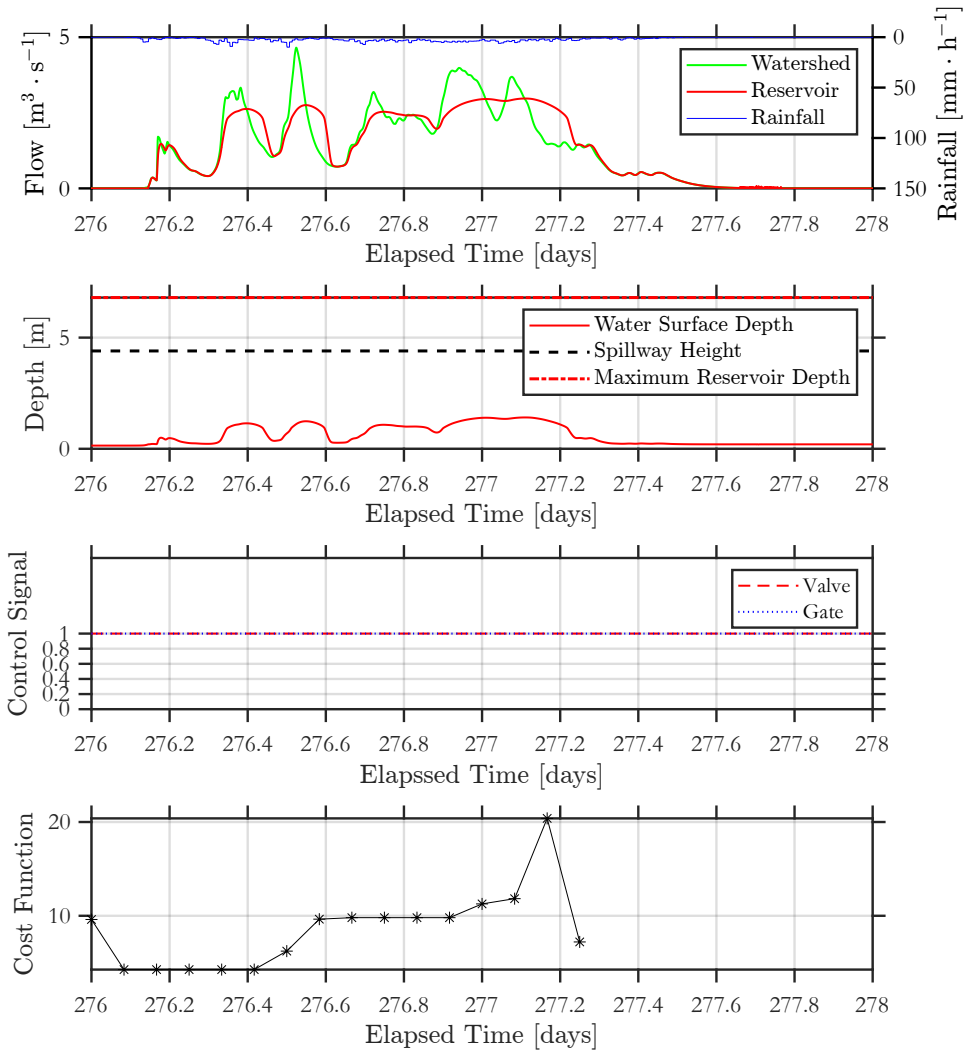

Figure 2: Continuous simulation results for day 276 to 278 of the passive scenario with valves fully opened corresponding to the minor flood event assessed.

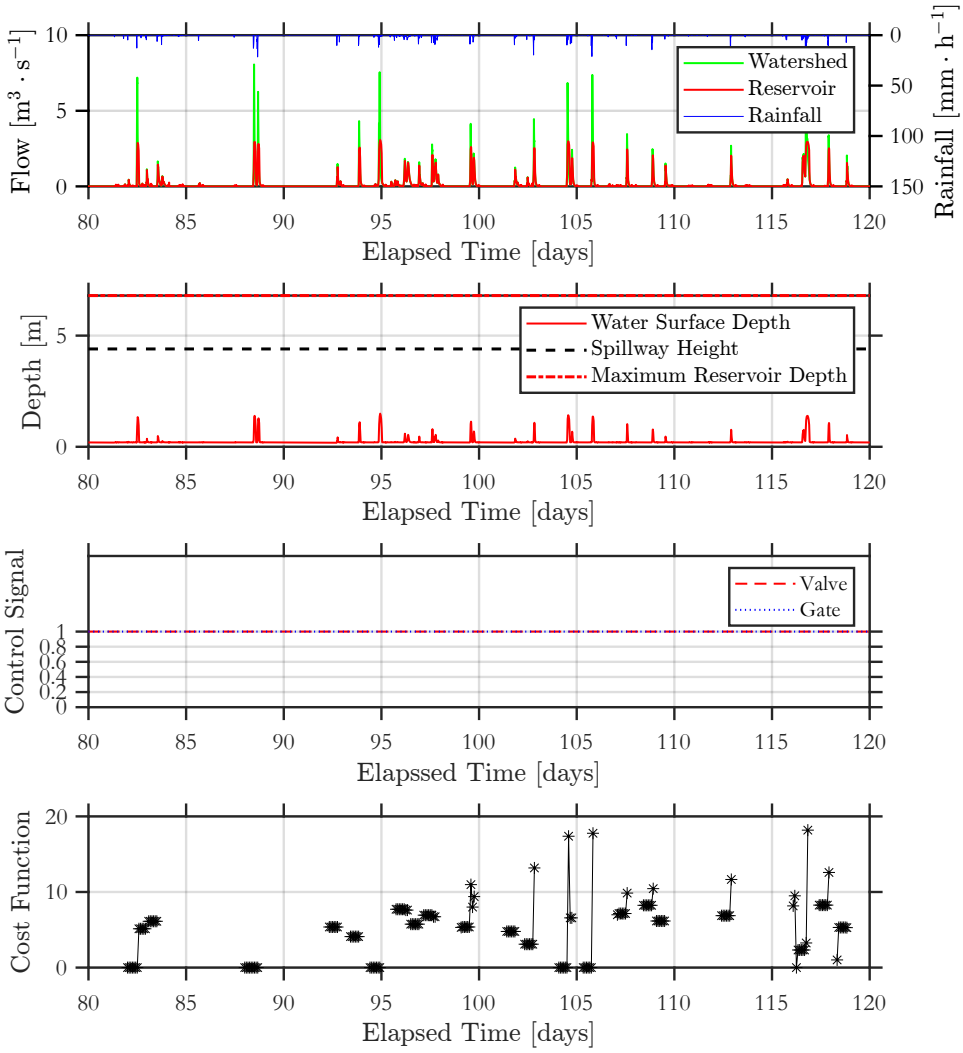

Figure 3: Continuous simulation results for day 80 to 120 of the passive scenario with valves fully opened corresponding to the minor flood event assessed.

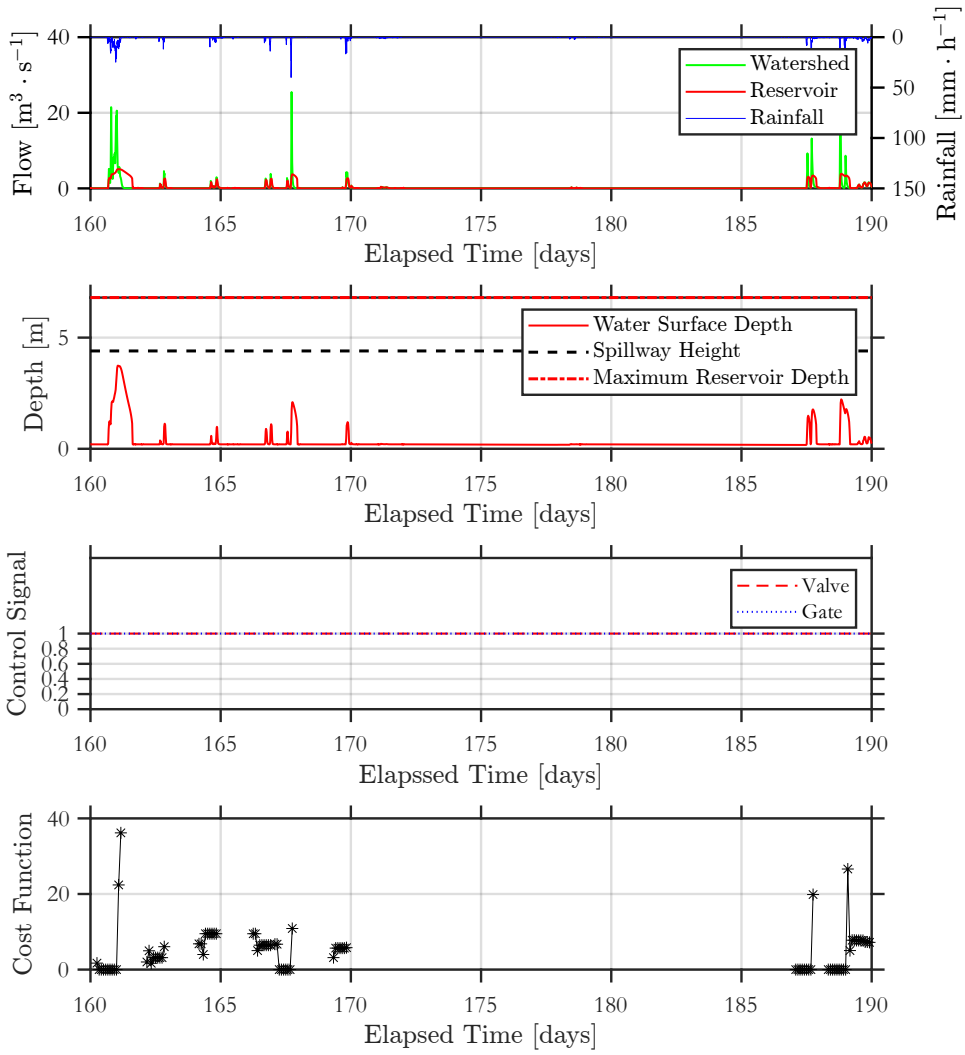

Figure 4: Continuous simulation results for day 160 to 190 of the passive scenario with valves fully opened corresponding to the minor flood event assessed.

Parameter	Description	Value	Unit
α_{s}^{g}	Gate exponent	1.5	-
b	Orifice width	1	m
c_{h}	Interval where controls are implemented	120	min
c_{i}	Interval where controls are performed	60	min
Δt_{max}	Maximum detention time allowed	18	h
k_{s}^{g}	Gate coefficient	27	-
l	Orifice height	1	m
$\mathrm{max_e}$	Maximum number of evaluations	120	-
$\mathrm{max_i}$	Maximum number of iterations per optimization problem	120	-
$\mathrm{max_{r,d}}$	Maximum reservoir water depth	6.8	m
$\mathrm{n_o}$	Number of orifices	1	-
$\mathrm{n_r}$	Number of initial randoms to start the optimization problem	5	-
Δp^{h}	Interval where predictions of future states are made	720	min
q_{*}^{t}	Threshold for releasing stored volume	2	$\mathrm{m^3 s^{-1}}$
q_{max}^{*}	Threshold for minor flooding	10	$\mathrm{m^3 s^{-1}}$
q_{max}^{**}	Threshold for large flooding	40	$\mathrm{m^3 s^{-1}}$
ρ_{r}	Weight for surpassing the maximum reservoir water depth	10^6	-
ρ_{u}	Weight for control effort	1	-
$h_{\mathrm{ref}}^{\mathrm{r}}$	Reference water level	6.8	m

Table 1: Input values for Numerical Case Study 3.

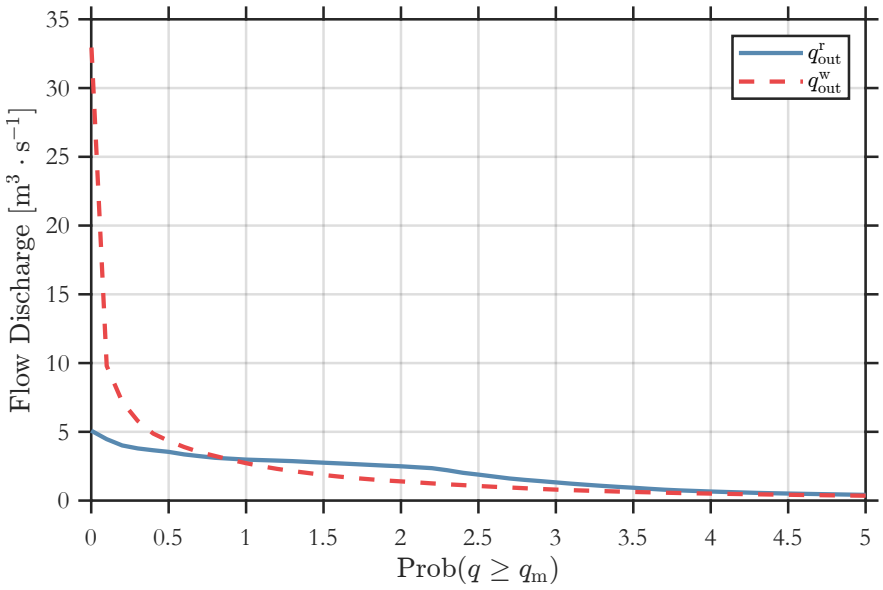

Figure 5: Duration curve of flow discharges for the reservoir with 100% of the valves opened.

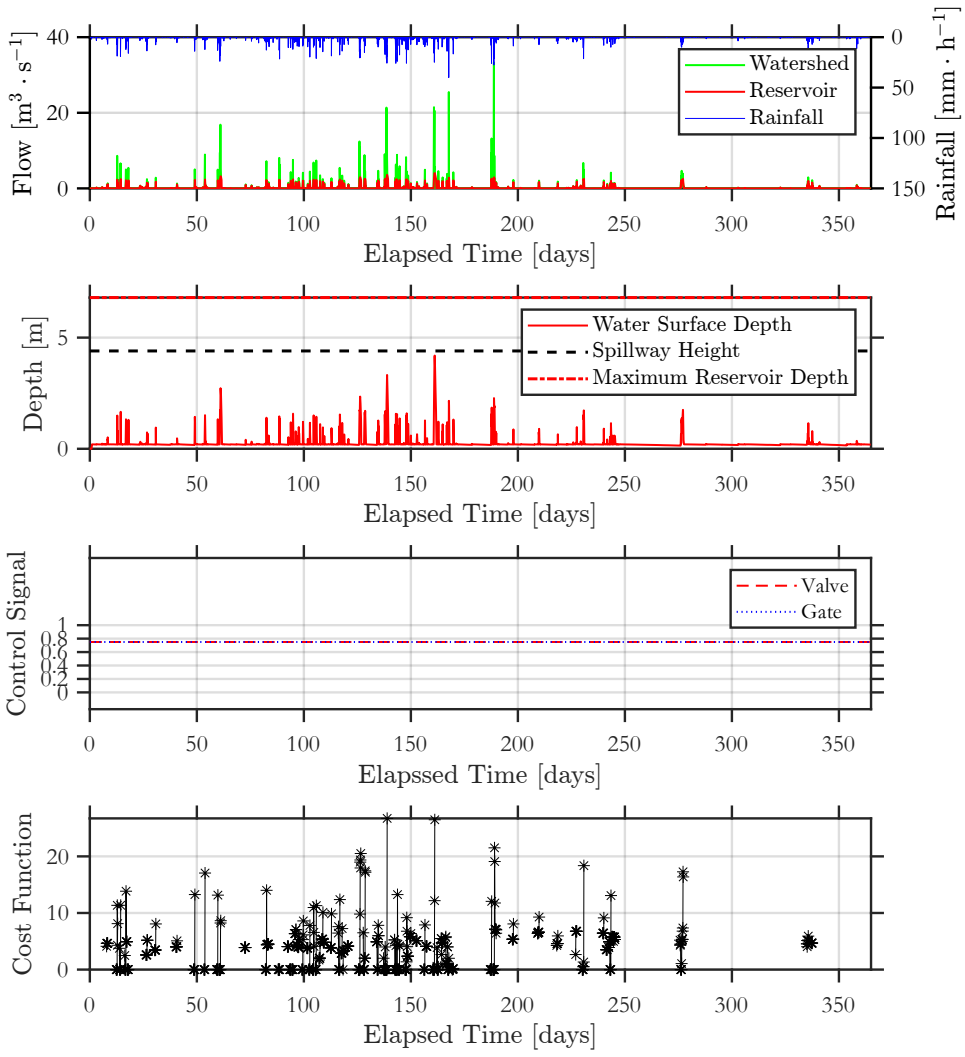

Figure 6: Continuous simulation results for day 1 to 365 of the passive scenario with valves 75% opened.

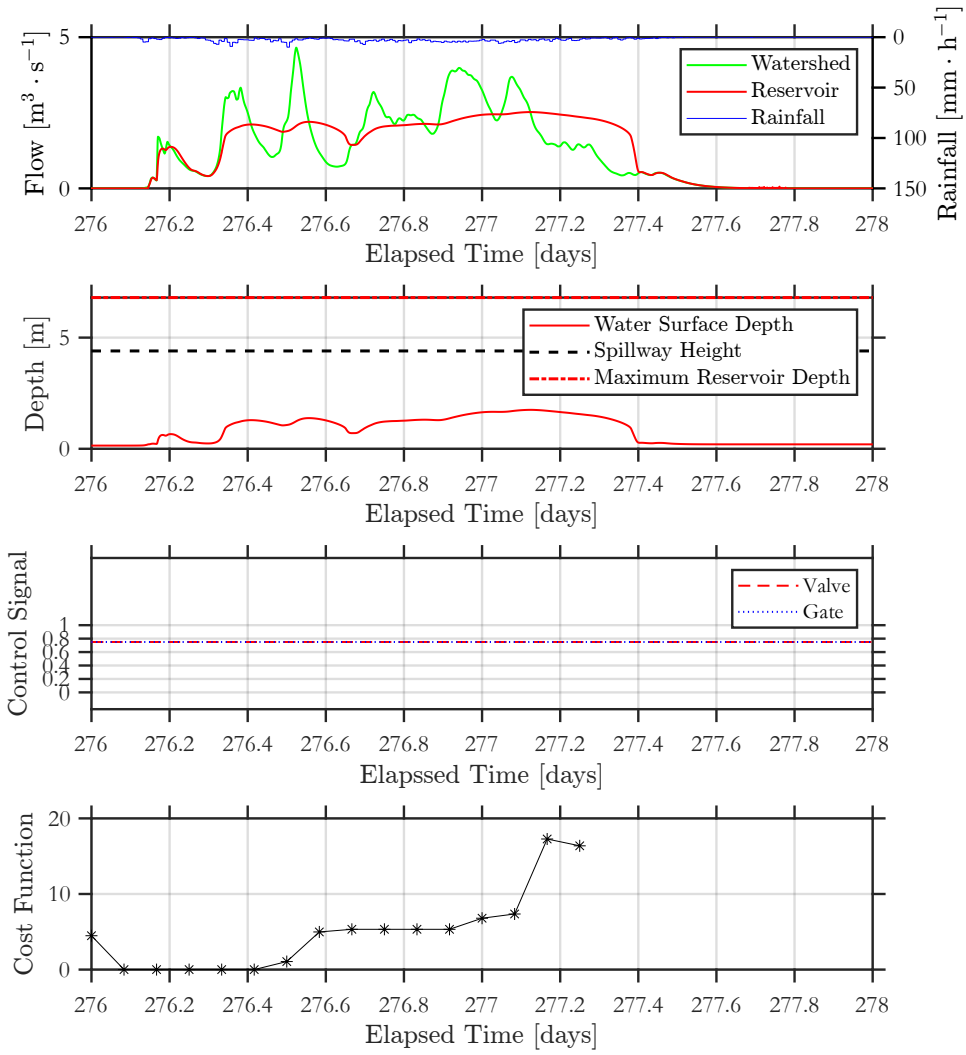

Figure 7: Continuous simulation results for day 276 to 278 of the passive scenario with valves 75% opened corresponding to the minor flood event assessed.

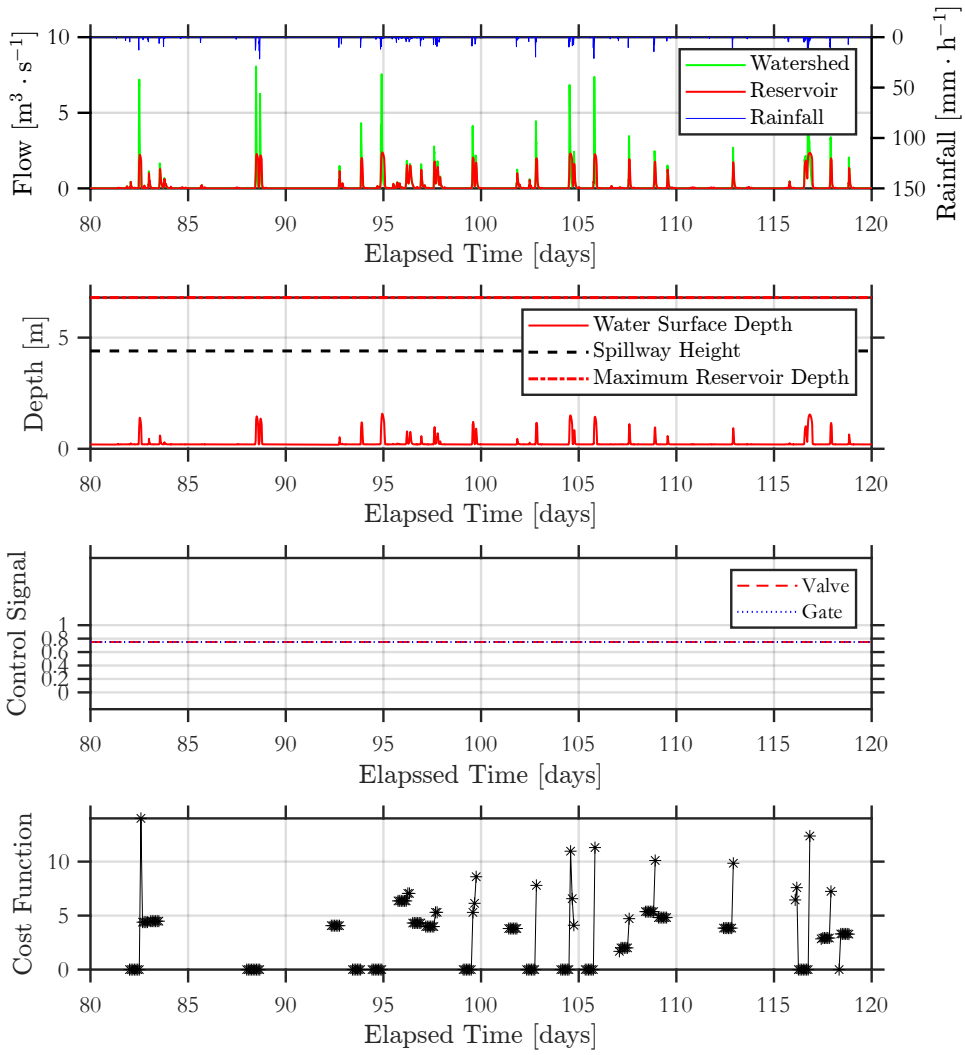

Figure 8: Continuous simulation results for day 80 to 120 of the passive scenario with valves 75% opened corresponding to the minor flood event assessed.

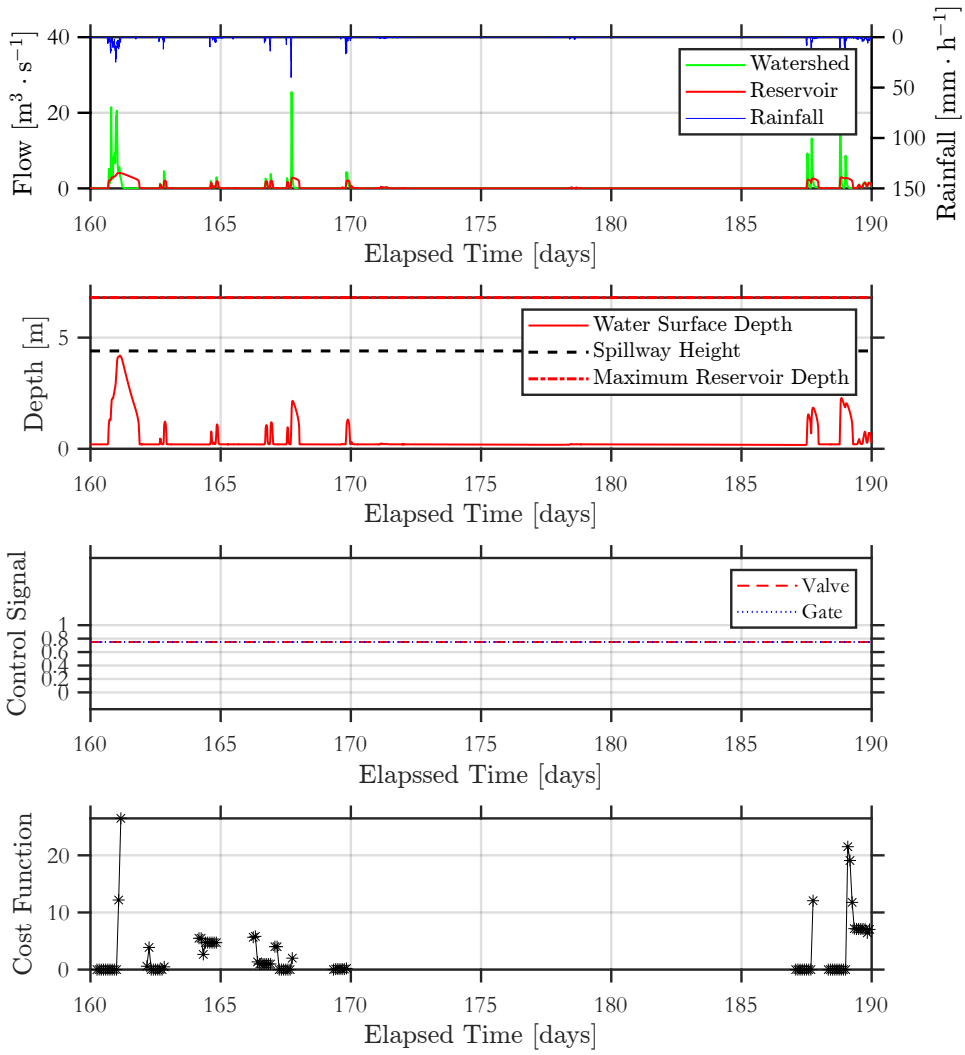

Figure 9: Continuous simulation results for day 160 to 190 of the passive scenario with valves 75% opened corresponding to the minor flood event assessed.

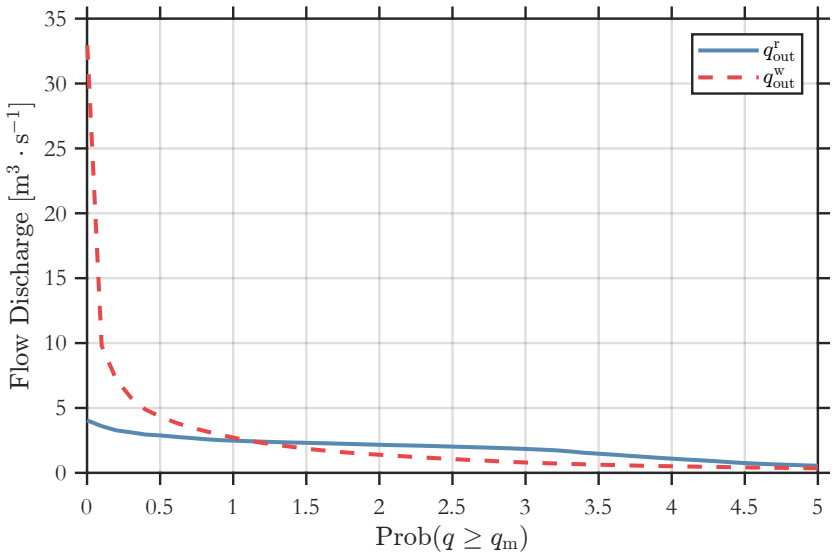

Figure 10: Duration curve of flow discharges for the reservoir with 75% of the valves opened.

1.9. 1-yr continuous simulation with the valve 75% opened

1.10. 1-yr continuous simulation with the valve 50% opened

1.11. 1-yr continuous simulation with the valve 25% opened

References

[1] W. H. Green, G. A. Ampt, Studies on soil phyics., The Journal of Agricultural Science 4 (1911) 1–24.

[2] P. C. Sentelhas, T. J. Gillespie, E. A. Santos, Evaluation of fao penman–monteith and alternative methods for estimating reference evapotranspiration with missing data in southern ontario, canada, Agricultural water management 97 (2010) 635–644.

[3] C. W. Thornthwaite, An approach toward a rational classification of climate, Geographical review 38 (1948) 55–94.

[4] G. H. Hargreaves, Z. A. Samani, Reference crop evapotranspiration from temperature, Applied engineering in agriculture 1 (1985) 96–99.

[5] R. G. Allen, M. E. Jensen, J. L. Wright, R. D. Burman, Operational estimates of reference evapotranspiration, Agronomy journal 81 (1989) 650–662.

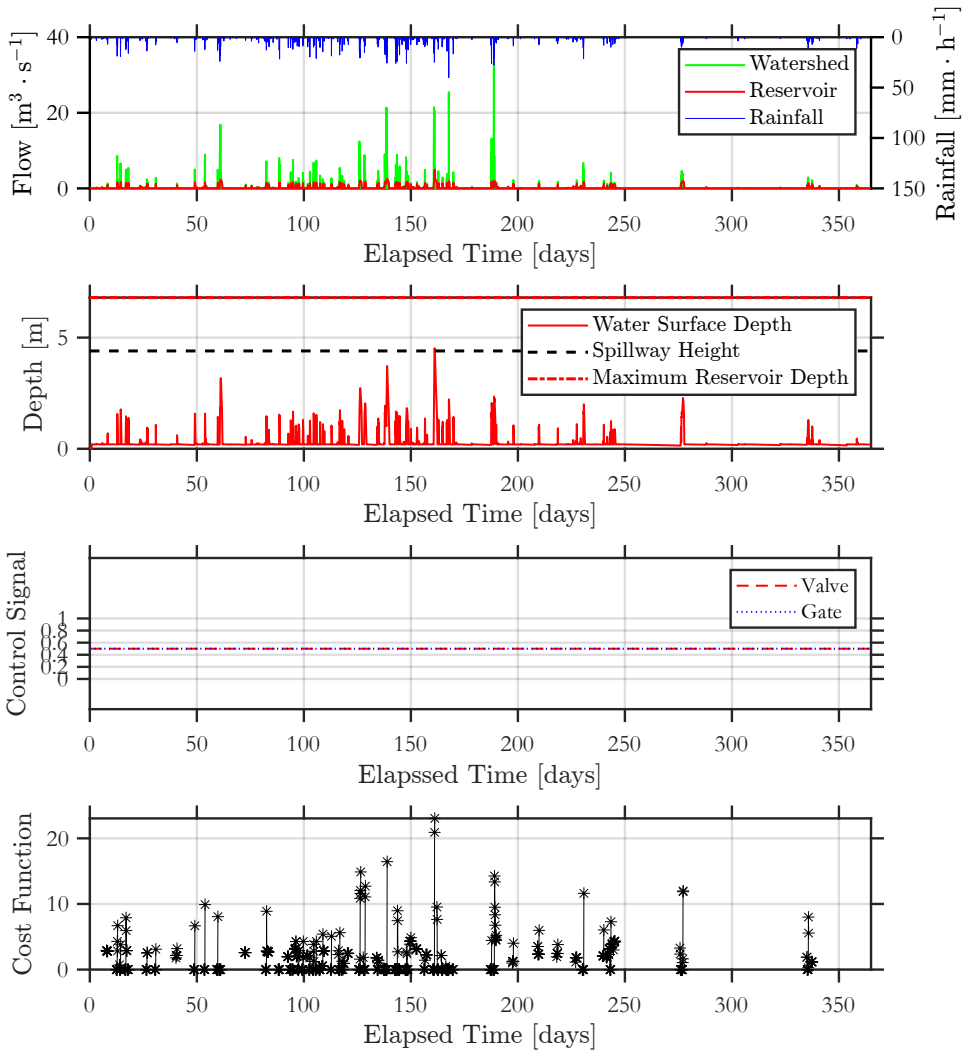

Figure 11: Continuous simulation results for day 1 to 365 of the passive scenario with valves 50% opened.

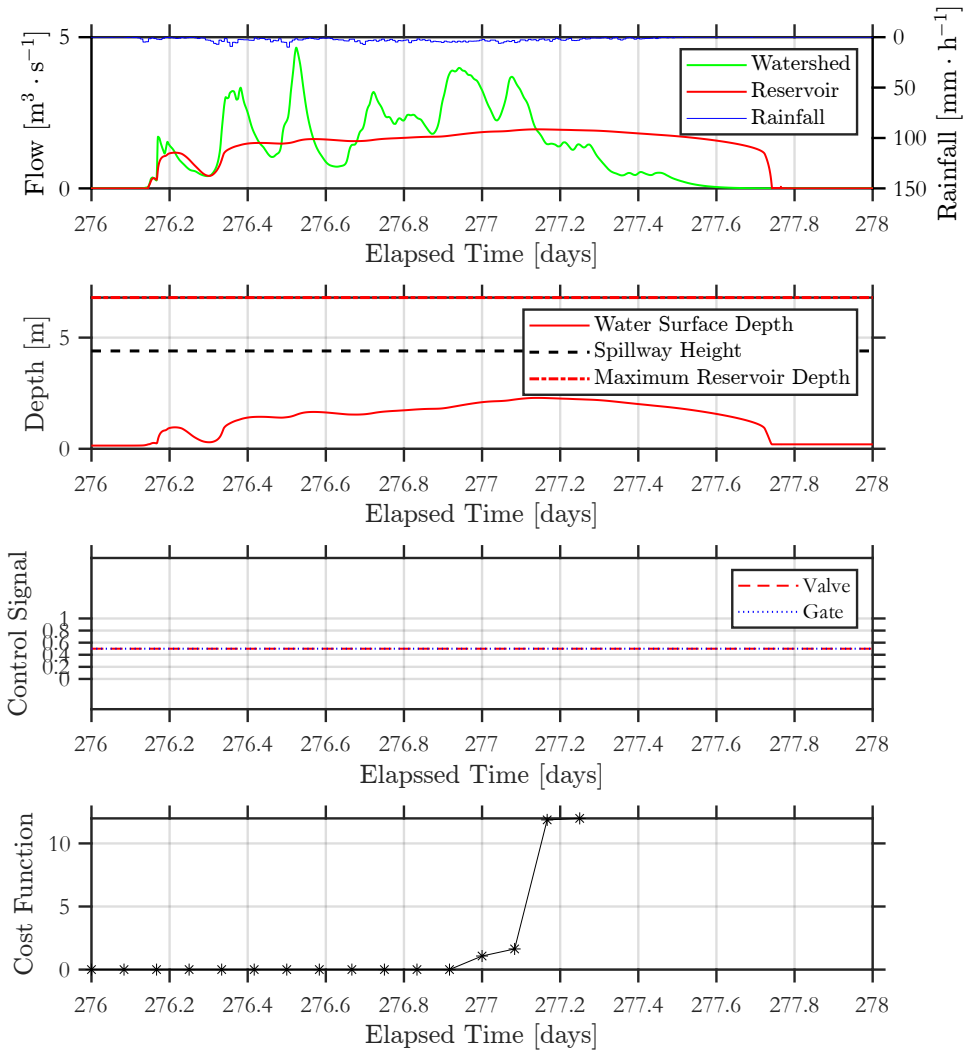

Figure 12: Continuous simulation results for day 276 to 278 of the passive scenario with valves 50% opened corresponding to the minor flood event assessed.

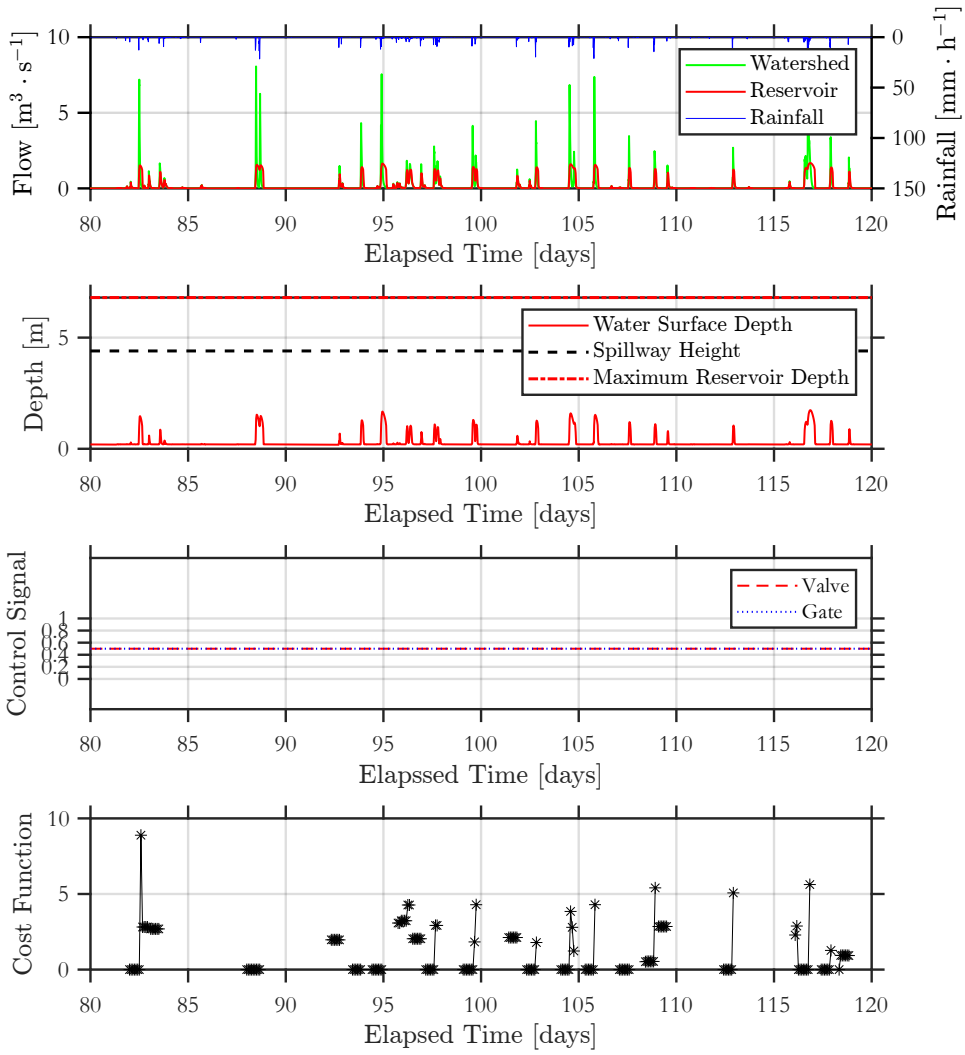

Figure 13: Continuous simulation results for day 80 to 120 of the passive scenario with valves 50% opened corresponding to the minor flood event assessed.

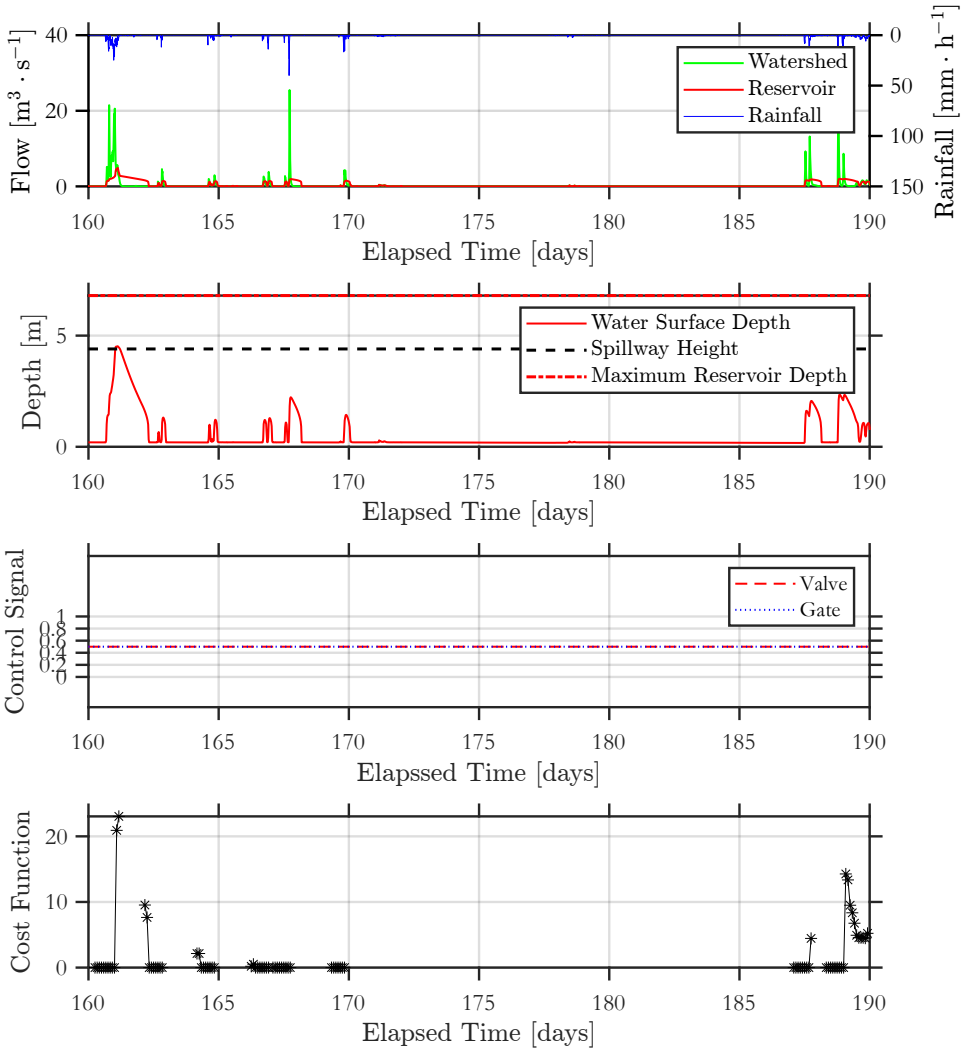

Figure 14: Continuous simulation results for day 160 to 190 of the passive scenario with valves 50% opened corresponding to the minor flood event assessed.

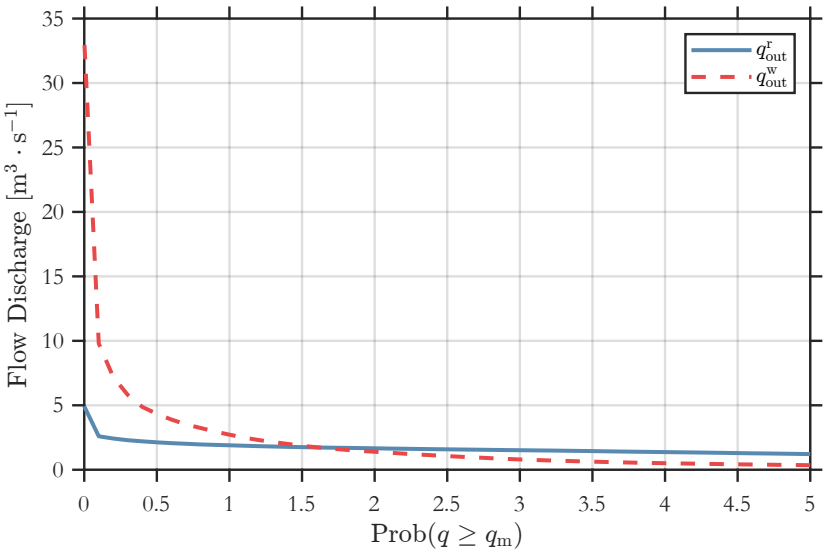

Figure 15: Duration curve of flow discharges for the reservoir with 50% of the valves opened.

[6] J. Cai, Y. Liu, T. Lei, L. S. Pereira, Estimating reference evapotranspiration with the fao penman–monteith equation using daily weather forecast messages, Agricultural and Forest Meteorology 145 (2007) 22–35.

[7] L. A. Rossman, Storm water management model user's manual, version 5.0, National Risk Management Research Laboratory, Office of Research and ..., 2010.

[8] P. M. Bartier, C. P. Keller, Multivariate interpolation to incorporate thematic surface data using inverse distance weighting (idw), Computers & Geosciences 22 (1996) 795–799.

[9] M. N. Gomes, C. A. F. do Lago, L. M. C. Rápalo, P. T. S. Oliveira, M. H. Giacomoni, E. M. Mendiondo, Hydropol2d — distributed hydrodynamic and water quality model: Challenges and opportunities in poorly-gauged catchments, Journal of Hydrology 625 (2023) 129982. URL: https://www.sciencedirect.com/science/article/pii/S0022169423009241. doi:https://doi.org/10.1016/j.jhydrol.2023.129982.

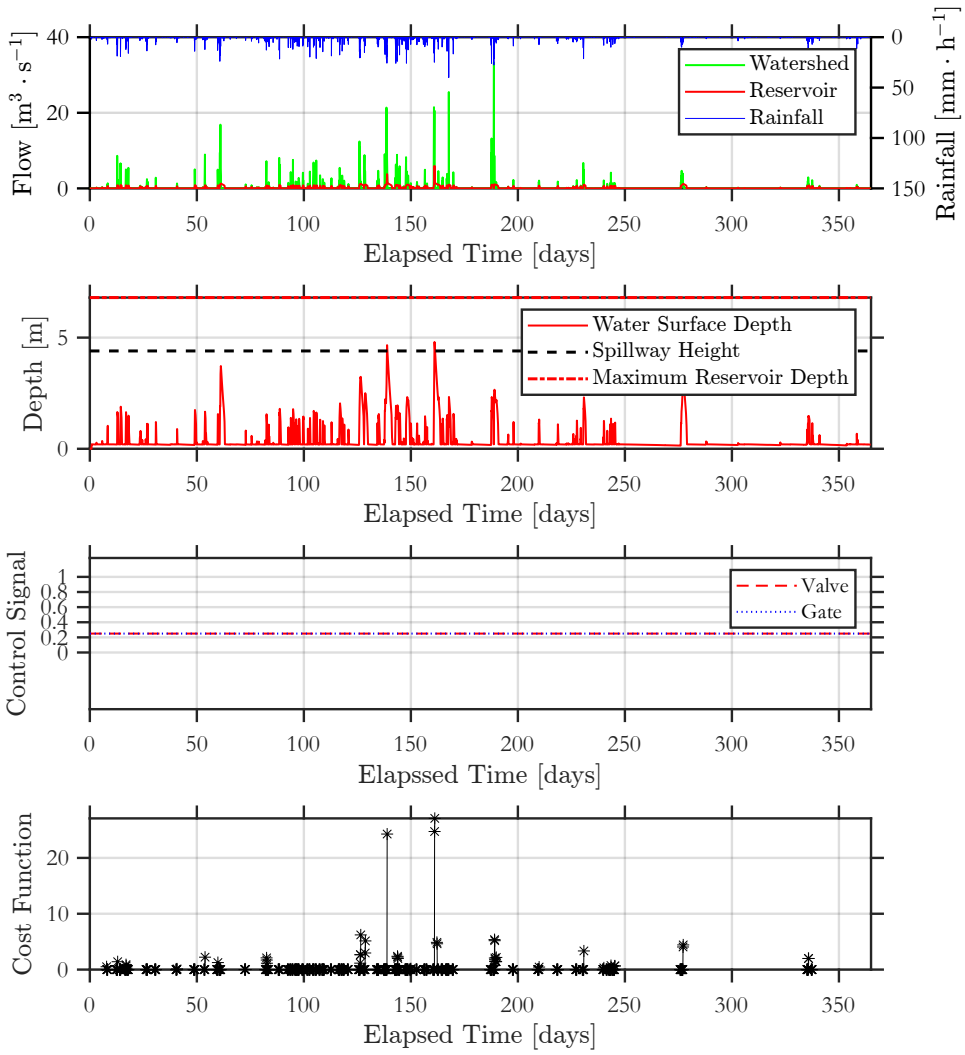

Figure 16: Continuous simulation results for day 1 to 365 of the passive scenario with valves 25% opened.

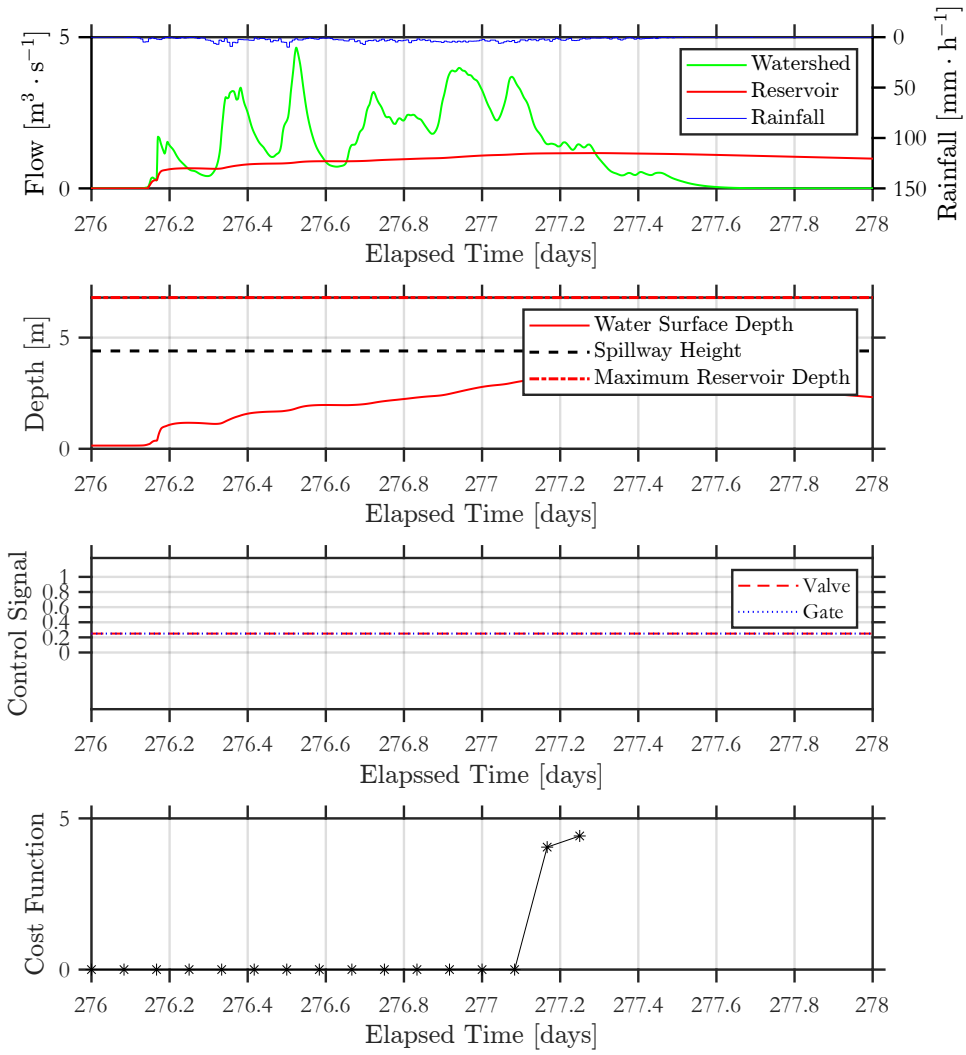

Figure 17: Continuous simulation results for day 276 to 278 of the passive scenario with valves 25% opened corresponding to the minor flood event assessed.

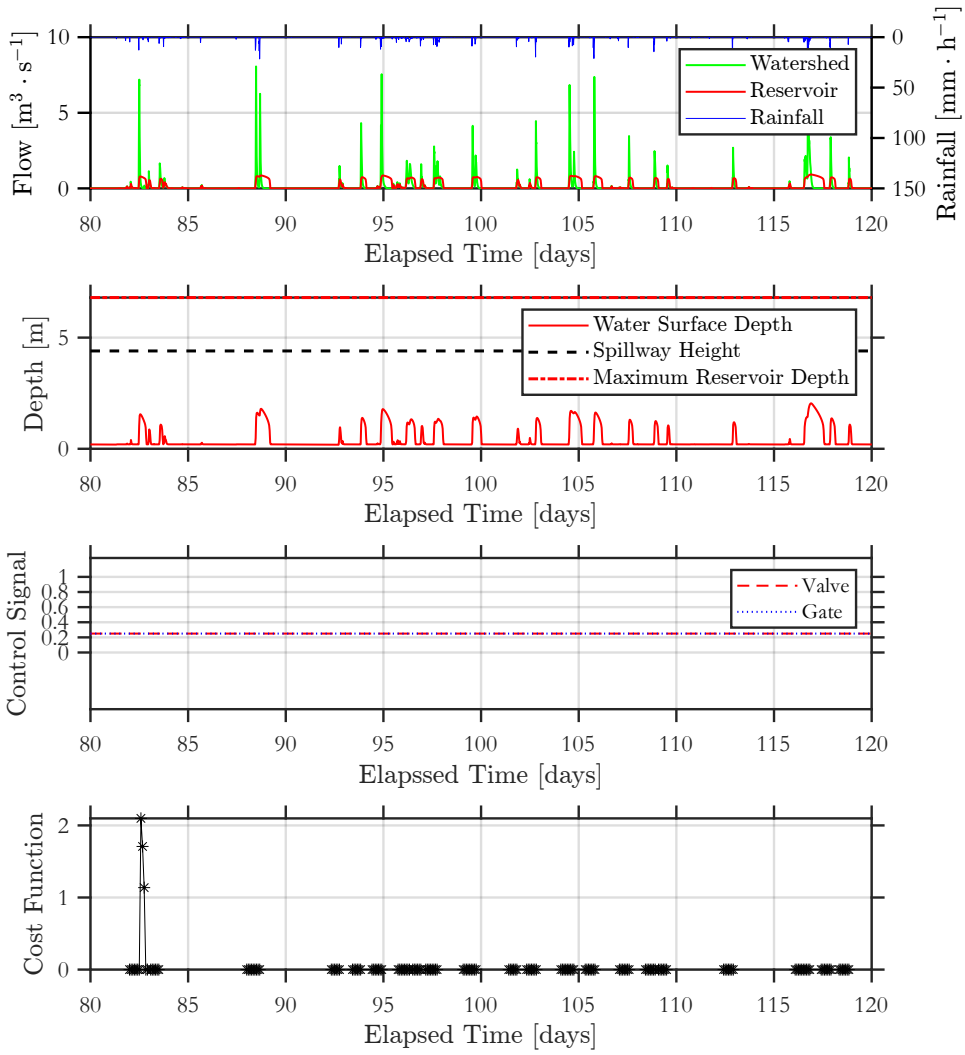

Figure 18: Continuous simulation results for day 80 to 120 of the passive scenario with valves 25% opened, corresponding to the minor flood event assessed.

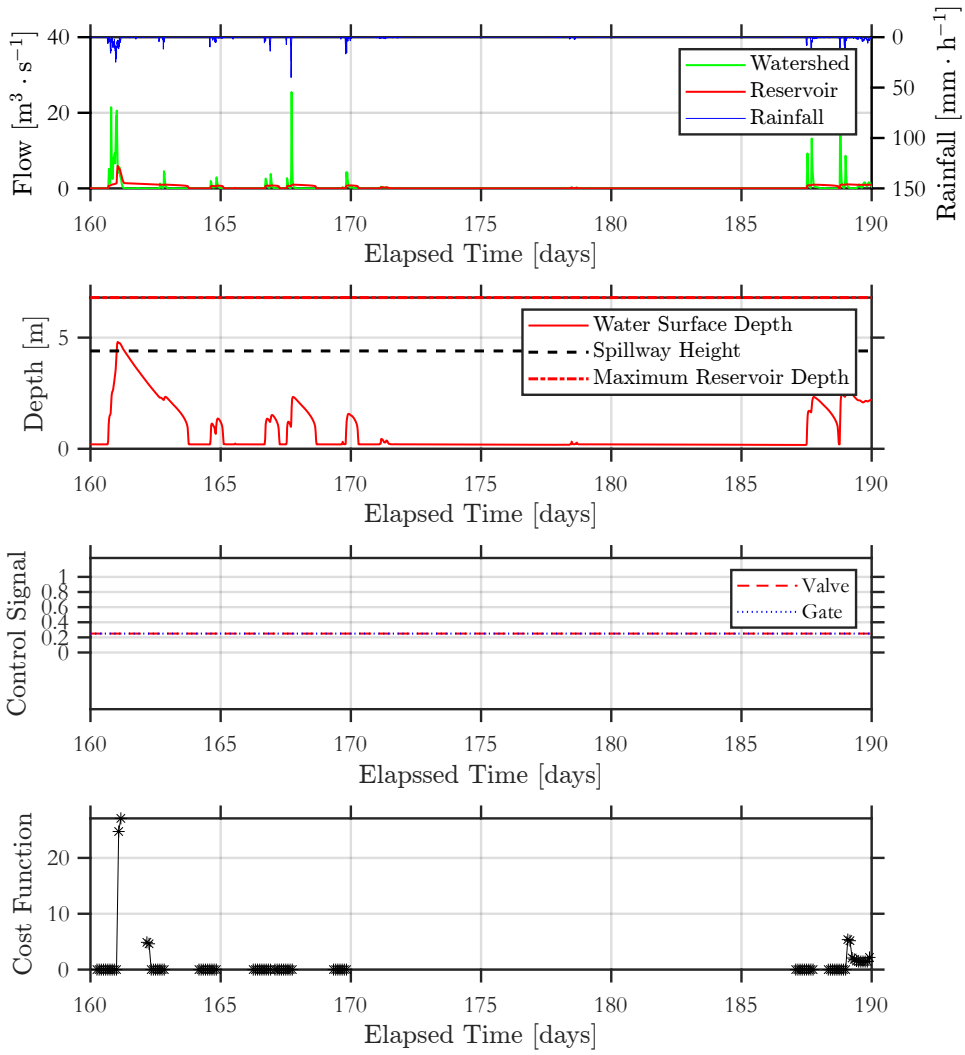

Figure 19: Continuous simulation results for day 160 to 190 of the passive scenario with valves 25% opened corresponding to the minor flood event assessed.

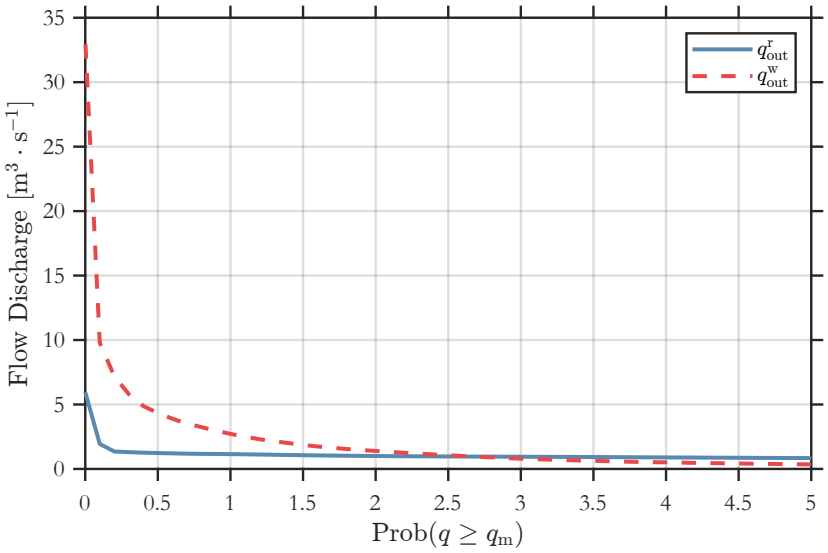

Figure 20: Duration curve of flow discharges for the reservoir with 25% of the valves opened.